THE ASTROPHYSICAL JOURNAL, 465:288–295, 1996 July 1

DISCOVERY OF O VI EMISSION FROM THE GALACTIC CORONA WITH THE HOPKINS ULTRAVIOLET TELESCOPE

W. VAN DYKE DIXON AND ARTHUR F. DAVIDSEN
Department of Physics and Astronomy, The Johns Hopkins University, Charles and 34th Streets, Baltimore, MD 21218; wvd@pha.jhu.edu, afd@pha.jhu.edu

AND

HENRY C. FERGUSON
Space Telescope Science Institute, Baltimore, MD 21218; ferguson@stsci.edu
Received 1995 September 25; accepted 1996 January 10

ABSTRACT

We have searched for far-UV emission from coronal gas in the Galactic halo along lines of sight with Galactic latitudes between 42° and 88° in spectra obtained by the Hopkins Ultraviolet Telescope during the Astro-2 space shuttle mission in 1995 March. Of four spectra taken through a 19″ × 197″ aperture, two show O VI λλ1032, 1038 emission at a significance of 4 σ. Two out of six spectra taken through a 10″ × 56″ aperture also show O VI emission, though at only 2 σ levels of significance. Three of the detections lie near regions of enhanced soft X-ray emission associated with Radio Loop I. The fourth, at $l = 218°$, $b = 56°$, may represent a more typical region of the halo. In its spectrum, we find $I(\mathrm{O\ VI}) = (3.59 \pm 0.96) \times 10^{-7}$ ergs cm^{-2} s^{-1}. This is the first detection of O VI emission from the Galactic halo. None of the spectra exhibit significant emission from C IV λλ1548, 1551, though our upper limits are greater than the intensities reported for other lines of sight. We set a limit on $I(\mathrm{O\ VI})/I(\mathrm{C\ IV}) \geq 3.4$, consistent with the predictions of self-photoionizing Galactic fountain models, but higher than those of models based on turbulent mixing layers. Combining our measured O VI intensity with estimates of N(O VI) through the halo, we find that, for $5.3 \leq \log T \leq 5.8$, the data are consistent with $n_e \approx 0.06$ cm^{-3} and $22{,}000 \leq P/k \leq 67{,}000$ cm^{-3} K, values substantially greater than those derived from C IV observations, suggesting that the C IV and O VI emission arise from physically distinct clouds and/or that a substantial portion of the C IV absorption arises from cooler gas that does not contribute to the C IV emission. This result is consistent with Galactic halo models incorporating self-photoionization of the cooling gas.

Subject headings: diffuse radiation — Galaxy: halo — ultraviolet: ISM

1. INTRODUCTION

The presence of hot gas in the Galactic halo was first postulated by Spitzer (1956) as a mechanism for confining the cool gas clouds seen high above the plane. This idea has since been extended into the "Galactic fountain" model, in which correlated supernovae in the disk eject 10^6 K gas into the halo, where it cools radiatively, loses buoyancy, and falls back toward the disk (Shapiro & Field 1976; Bregman 1980; Norman & Ikeuchi 1989). Direct evidence of hot gas in the halo comes from observations of interstellar O VI, N V, Si IV, and C IV absorption in ultraviolet spectra of halo stars and extragalactic objects (Sembach & Savage 1992; Savage et al. 1993; Davidsen 1993; Hurwitz et al. 1995). As the gas cools through 10^5 K, it should emit strongly in the O VI λλ1032, 1038, N V λλ1239, 1243, and C IV λλ1548, 1551 resonance lines (Voit, Donahue, & Slavin 1994). Emission from C IV at high Galactic latitude has been detected by Martin & Bowyer (1990), while upper limits on the diffuse O VI coronal emission have been set by Dixon et al. (1993) and Edelstein & Bowyer (1993).

A variety of cooling models have been suggested to account for these results. Among them are models in which hot halo gas undergoes isobaric (constant pressure) or isochoric (constant density) cooling (Edgar & Chevalier 1986), models which incorporate self-photoionization of the cooling gas (Benjamin & Shapiro 1996), and models incorporating turbulent mixing layers and isobarically cooling supernova remnants (Shull & Slavin 1994). In principle, observations of O VI and X-ray emission can discriminate among these models (McKee 1993). To this end, we have used the Hopkins Ultraviolet Telescope (HUT) to conduct a search for diffuse O VI emission from coronal gas in the Galactic halo.

2. OBSERVATIONS AND DATA REDUCTION

Our observations were carried out with HUT on the Astro-2 mission of the space shuttle *Endeavour* in 1995 March. HUT consists of a 0.9 m, f/2 mirror that feeds a prime-focus spectrograph with a microchannel-plate intensifier and photodiode array detector. First-order sensitivity extends from 820 to 1840 Å at 0.51 Å pixel^{-1}. The resolution is about 4 Å through the spectrograph's 10″ × 56″ aperture and 7 Å through its 19″ × 197″ aperture. Though the telescope was not originally designed to measure the far-UV background, improvements to its mirror and grating coatings have raised its effective area to nearly 24 cm^2 at 1032 Å, making detection of O VI λλ1032, 1038 emission a possibility. The spectrograph and telescope are described by Davidsen et al. (1992), while Kruk et al. (1995) discuss modifications, performance, and calibration for the Astro-2 mission.

Of the 265 targets observed during the mission, 10 were chosen for detailed analysis according to the following criteria: their spectra were obtained using the largest apertures of the HUT spectrograph, thus maximizing the flux from diffuse coronal emission; they show little or no continuum emission; and they were observed during orbital night, eliminating the O I airglow features at 1027 and 1040 Å and

TABLE 1

TARGET SUMMARY

Number	Name	R.A.(1950)	Decl.(1950)	l	b	GMT of Start	Time (s)	Slit[a]	Comments
1.....	UGC 6151	11:03:16.00	+20:05:40.00	224.1	64.8	062:23:50:17	952	5	No observed continuum
2.....	VCC 2037	12:43:43.00	+10:28:48.00	298.5	73.0	064:04:57:19	472	5	No object in slit
						068:06:16:04	1508	5	
3.....	UGC 5675	10:25:39.00	+19:48:24.00	218.2	56.4	072:09:15:29	2044	5	No object in slit[b]
4.....	IC 2574	10:24:41.30	+68:40:18.00	140.2	43.6	075:02:52:39	950	5	Strong Lyα scattering
5.....	SA 57	13:06:15.61	+29:40:29.89	65.0	85.6	065:17:29:34	750	6	No object in slit
6.....	NGC 4038	11:59:19.00	−18:35:12.00	287.0	42.5	066:05:23:26	1918	6	No observed continuum
7.....	VCC 530	12:19:45.00	+16:04:42.00	270.6	76.8	068:20:27:56	1844	6	No object in slit[b]
8.....	NGC 4631	12:39:39.76	+32:47:30.00	143.0	84.2	069:14:12:52	2052	6	Pointed at halo; continuum present
						071:16:25:07	2634	6	
9.....	HER-CLUS	16:03:12.00	+17:57:00.00	31.7	44.5	069:20:23:56	1592	6	No object in slit
						072:20:05:01	1592	6	
10.....	AB 1795	13:46:33.94	+26:50:27.60	33.8	77.2	072:21:26:47	2346	6	Faint continuum

[a] Slit 5 measures 19″ × 197″; slit 6 is 10″ × 56″.
[b] Aperture was offset 2′ from galaxy center.

minimizing the strength of the Lyβ airglow line and the scattered light from Lyα, which is quite strong during the day. Table 1 lists the observations in our sample. Although each target was assigned the name of a nearby astronomical object, many are actually offsets from faint galaxies or blank-sky pointings. Three of the targets were observed twice; their spectra were added together for our analysis.

In our analysis, models are fitted to raw-counts spectra using the nonlinear curve-fitting program SPECFIT (Kriss 1994), which runs in the IRAF[1] environment and performs a χ^2 minimization. Error bars are assigned to the data assuming Poisson statistics. Emission-line intensities are converted to energy units using the HUT absolute calibration, which is based on white dwarf model atmospheres and is believed accurate to about 5% (Kruk et al. 1995). Throughout this paper, line intensities and ratios are expressed in units of ergs cm^{-2} s^{-1} sr^{-1}.

Because the O VI lines lie within the wings of the Lyβ airglow feature, it is crucial that we accurately model the Lyβ line profile and extended wings. Unfortunately, there are no obvious templates for such a model. Except for the Lyβ and Lyα lines, all of the strong airglow lines in the HUT spectral region are broadened by multiple components. Lyβ line profiles obtained during the daylight portion of an orbit, for which the O VI contribution would be insignificant, are not available because detector safety concerns prevented use of the 19″ × 197″ aperture during such periods. The Lyα line cannot be used as the basis for a model line profile because its intense flux effectively "scrubbed" the microchannel-plate intensifier system throughout the mission, producing a distorted and time-dependent line profile (Kruk et al. 1995).

We therefore build a model airglow line profile, beginning with a point-source emission feature, the He II λ1640 line from the HUT spectrum of Z And presented in Figure 1. A linear model is fitted to the nearby stellar continuum and subtracted from the data. The wings of the line, which have few counts, are fitted with a cubic spline function, then replaced by it. The 19″ × 197″ aperture, when projected onto the HUT detector, spans 6.9 Å; our model is thus convolved with a square wave of this width. Finally, because the instrumental resolution varies with wavelength (Kruk et al. 1995), the model is broadened with a Gaussian line profile. The width of the Gaussian is determined empirically by convolving the model with a series of Gaussians and comparing the result with an observed spectrum, the sum of several large-aperture observations. The best fit is found using a Gaussian of FWHM = 1.8 Å. A model emission-line profile for the 10″ × 56″ aperture is developed in the same way, using a square wave 3.6 Å wide.

To search for O VI emission, we fit a linear continuum and three emission features, Lyβ λ1026 and O VI λλ1032,

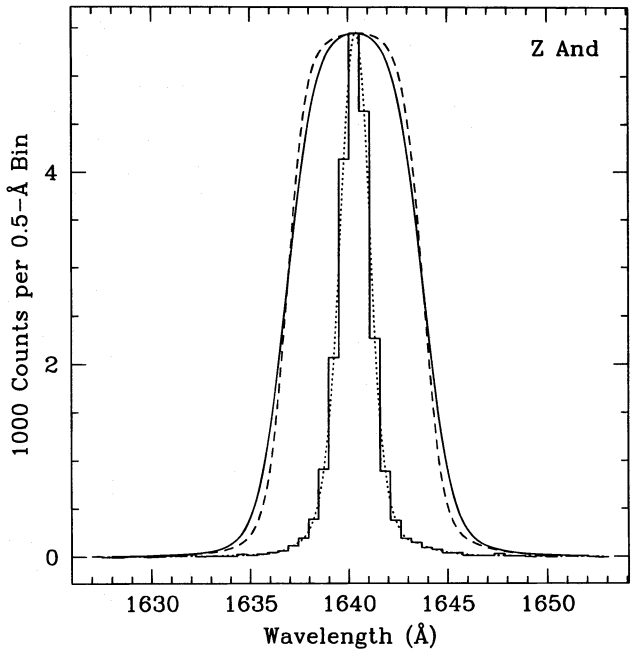

FIG. 1.—Continuum-subtracted spectrum of Z And showing the He II λ1640 emission feature (histogram) that was used as the basis for our model Lyβ line profile. The wings of this line, which have few counts, were fitted with a spline curve and replaced (*dotted line*). The profile was convolved with a square wave of width 6.9 Å (*dashed line*) to model the 19″ × 197″ aperture, then with a Gaussian of FWHM = 1.8 Å to match the instrument resolution at 1026 Å (*solid line*).

[1] The Image Reduction and Analysis Facility (IRAF) is distributed by the National Optical Astronomy Observatories, which is operated by the Association of Universities for Research in Astronomy, Inc. (AURA), under cooperative agreement with the National Science Foundation.

1038, to a 165 pixel region of each raw-counts spectrum. Because the O VI lines are expected to fill the aperture, the same profile is used for them as for Lyβ. The wavelength of the Lyβ line is free to vary; those of the O VI lines are tied to it assuming the relative laboratory wavelengths. The line strengths also vary freely, except that the O VI lines are held to the 2:1 ratio expected from an optically thin plasma. The O VI line is then fixed at zero counts and the spectrum refitted. If $\Delta\chi^2 > 4$ (corresponding to a 2 σ deviation for one interesting parameter, in this case the total counts in the O VI line; Avni 1976), we claim a detection and determine 1 σ error bars by raising the model line strength above the best-fit level until $\Delta\chi^2 = 1$. Otherwise, we raise the model line strength above zero until $\Delta\chi^2 = 4$ and call this our 2 σ upper limit.

Our results are presented in Table 2. We detect O VI emission at a significance of 4 σ in two spectra obtained through the 19″ × 197″ aperture and at 2 σ in two spectra obtained through the 10″ × 56″ aperture. These are the first detections of O VI emission from the Galactic halo. The spectrum of the target UGC 5675, a position 2′ west of the center of this low surface brightness galaxy, is presented in Figure 2. The basis for our O VI detection is the clear asymmetry in the terrestrial Lyβ profile, which is not seen in all spectra and is well fitted by emission from the O VI doublet assuming our model line profile. The spectrum of UGC 6151, which does not show significant O VI emission, is presented in Figure 3. We see that our model airglow line profile successfully reproduces the Lyβ feature in both spectra, fitting the red wing of Lyβ in UGC 6151 and the blue wing in both spectra. The quality of the fit is reflected in the resulting values of χ^2, which are near 1.0 per degree of freedom for all but one of the fits listed in Table 2.

We use the same technique to set upper limits on the flux of the following emission features: C III λ977, C II λ1336, the Si IV–O IV] complex at 1400 Å, C IV $\lambda\lambda$1548, 1551, He II λ1640, and O III] $\lambda\lambda$1661, 1666. Our results are presented in Table 3; none of the spectra show significant emission in these lines.

Have we discovered O VI emission from the Galactic corona? We consider several alternative explanations for the emission observed at 1032–1038 Å. Broad O I airglow lines at 1027 and 1040 Å are generally present in HUT spectra obtained during orbital day but are absent in orbital-night spectra. These features are expected to be about 20 times weaker than the O I feature at 989 Å (Feldman et al. 1992; Feldman 1995). In the four targets for which we have positive detections of O VI, the data are consistent with zero flux in both the 989 and 1040 Å lines. We expect the contribution from the O I λ1027 feature, which is buried under the Lyβ line, to be negligible as well.

Emission at these wavelengths might be attributed to a poorly modeled bump in the wings of the Lyβ airglow line. If this were the case, we would expect its flux to scale with

TABLE 2

O IV INTENSITIES AND 2 σ UPPER LIMITS

Number	Name	Time (s)	χ^2/ν[a]	Counts[b]	Intensity[c]	Significance
1.....	UGC 6151	952	202.3/163	24.18	$\leq$4.75	...
2.....	VCC 2037	1980	138.3/162	38.64	4.03 $\pm$ 1.05	3.8 σ
3.....	UGC 5675	2044	152.6/162	33.86	3.59 $\pm$ 0.96	3.6 σ
4.....	IC 2574	950	162.6/163	18.54	$\leq$4.27	...
5.....	SA 57	750	139.9/163	4.20	$\leq$7.68	...
6.....	NGC 4038	1918	150.3/162	9.77	6.94 $\pm$ 3.29	2.1 σ
7.....	VCC 530	1844	139.6/163	2.94	$\leq$2.27	...
8.....	NGC 4631	4686	156.6/144	11.57	$\leq$3.55	...
9.....	HER-CLUS	3184	128.2/162	9.84	4.46 $\pm$ 2.25	2.0 σ
10.....	AB 1795	2346	161.7/163	13.52	$\leq$8.36	...

[a] For detections, χ^2 refers to the model including the best-fitting O VI flux; for upper limits, to the fit with no O VI.

[b] Raw counts in measured line or 2 σ upper limit.

[c] Units are 10^{-7} ergs cm^{-2} s^{-1} sr^{-1}.

TABLE 3

2 σ UPPER LIMITS TO FAR-UV EMISSION LINES

Number	Name	C III λ977	C II λ1336	Si IV, O IV][a]	C IV $\lambda\lambda$1548, 1551	He II λ1640	O III] $\lambda\lambda$1661, 1666
1.....	UGC 6151	0.93	2.08	5.39	0.91	1.32	1.63
2.....	VCC 2037	1.36	1.29	1.71	0.82	1.85	1.53
3.....	UGC 5675	1.69	1.85	1.26	1.07	0.68	2.34
4.....	IC 2574	3.18	1.03	6.14	2.22	6.02	2.62
5.....	SA 57	4.91	5.69	11.54	2.26	3.36	16.73
6.....	NGC 4038	3.44	4.90	5.12	4.42	4.07	4.93
7.....	VCC 530	6.58	3.28	6.77	5.91	1.58	9.19
8.....	NGC 4631	1.64	1.24	5.70	2.86	1.98	7.04
9.....	HER-CLUS	5.78	4.22	2.68	5.26	1.90	6.84
10.....	AB 1795	4.62	4.26	11.75	5.42	1.56	2.11
	Mean	3.41	2.98	5.80	3.11	2.43	5.50

[a] Complex of lines near 1400 Å modeled as two lines of equal strength at 1394 and 1403 Å, consistent with the log $\bar{T} = 5.3$, $v = 100$ km s^{-1} model of Slavin et al. 1993.

NOTE.—Units are 10^{-7} ergs cm^{-2} s^{-1} sr^{-1}.

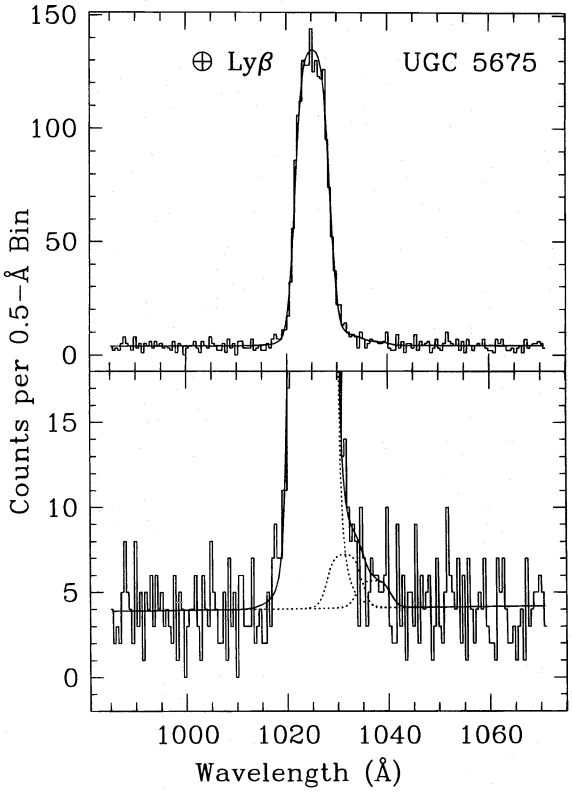

FIG. 2.—HUT spectrum of UGC 5675, in which O VI λλ1032, 1038 emission is present at a significance of 3.6 σ. The data are shown as a histogram and are overplotted by the best-fitting model, which includes emission in the O VI λλ1032, 1038 doublet. The composite model is plotted as a solid line. In the lower panel, the individual components are shown by dotted lines. The basis for our O VI detection is the clear asymmetry in the terrestrial Lyβ profile, which is not seen in all observations and is well fit by emission from the O VI doublet at the instrumental resolution.

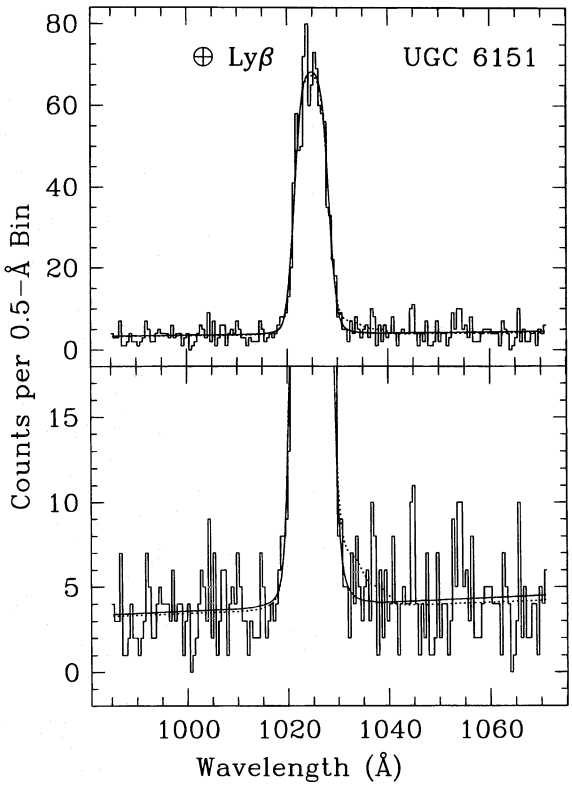

FIG. 3.—HUT spectrum of UGC 6151, which does not show significant O VI λλ1032, 1038 emission. The data are shown as a histogram; overplotted are models including no O VI λλ1032, 1038 emission (*solid line*) and O VI at our 2 σ upper limit (*dotted line*).

Lyβ. To test this, we divide the UGC 5675 observation, which was obtained in a single pointing, into two spectra. The first consists of data taken during the darkest 1000 s of orbital night (determined from the flux in the Lyα line). The second, also consisting of 1000 s of data, is essentially the rest of the observation. The Lyβ flux differs by a factor of 2.2 ± 0.1 between the two spectra, while the O VI flux is constant (0.7 ± 0.5) and consistent with that measured for the complete observation. We conclude that the observed O VI emission is real and not of terrestrial origin.

A third possibility is emission from C II λ1037, which could arise from cooler gas along the line of sight. Shock models do not predict significant flux in this line (it is not included in the line list of Hartigan, Raymond, & Hartmann 1987, for example), and the cooling-flow models of Benjamin & Shapiro (1986) predict the line to be only one-tenth as strong as the C II λ1336 feature, from which we see no significant emission in any of our spectra (Table 3).

We do not expect significant line emission at O VI wavelengths from extragalactic background sources. The spectra in our sample show little or no continuum emission, and many are blank-sky observations. Of the four spectra showing significant O VI emission (Table 2), only for target 6, NGC 4038, did an object actually fall in the HUT aperture. Its velocity, $cz = 1642 \pm 12$ km s^{-1} (Lauberts & Valentijn 1989), corresponds to a redshift of 5.7 Å at the wavelength of O VI, placing the redshifted 1032 Å feature close to the Galactic 1038 Å line. We find that adding a second O VI doublet at this redshift does not significantly improve χ^2.

O VI absorption has been seen in the spectra of halo stars and extragalactic objects (Jenkins 1978; Davidsen 1993; Hurwitz et al. 1995). If this gas were optically thick (a possibility discussed in § 3), what fraction of the observed O VI emission could be backscattered from supernova remnants in the disk? If we assume that there are about 200 supernova remnants in the Galaxy (Green 1991), distributed evenly over a disk of radius 15 kpc and each with an O VI luminosity of 5×10^{36} ergs s^{-1} (Cygnus Loop; Blair et al. 1991), then we derive a mean O VI surface brightness on either side of the disk of about 2×10^{-8} ergs cm^{-2} s^{-1} sr^{-1}, roughly 5% of our observed O VI intensity (Table 2). We conclude that backscattering from supernova remnants contributes negligibly to the observed O VI emission.

It is more likely that our line of sight is affected by a single nearby supernova remnant. Figure 4 is a map of the north Galactic pole showing the location of each of the targets in our survey. Also plotted is the M-band (490–1190 eV) X-ray intensity map of McCammon et al. (1983). The prominent emission feature is Radio Loop I, thought to be gas shock-heated to 10^6 K in the outer shell of a supernova remnant (Iwan 1980; Heiles et al. 1980). We see that three of the four HUT targets yielding positive detections of O VI emission, Nos. 2, 6, and 9, lie on or near this feature. While detection of O VI emission from Radio Loop I is itself an interesting result, a discussion of its implications is beyond the scope of this paper. In any case, this correlation lends credibility to our results. The line of sight to target 3, UGC 5675, probes a more quiescent region of the X-ray sky and

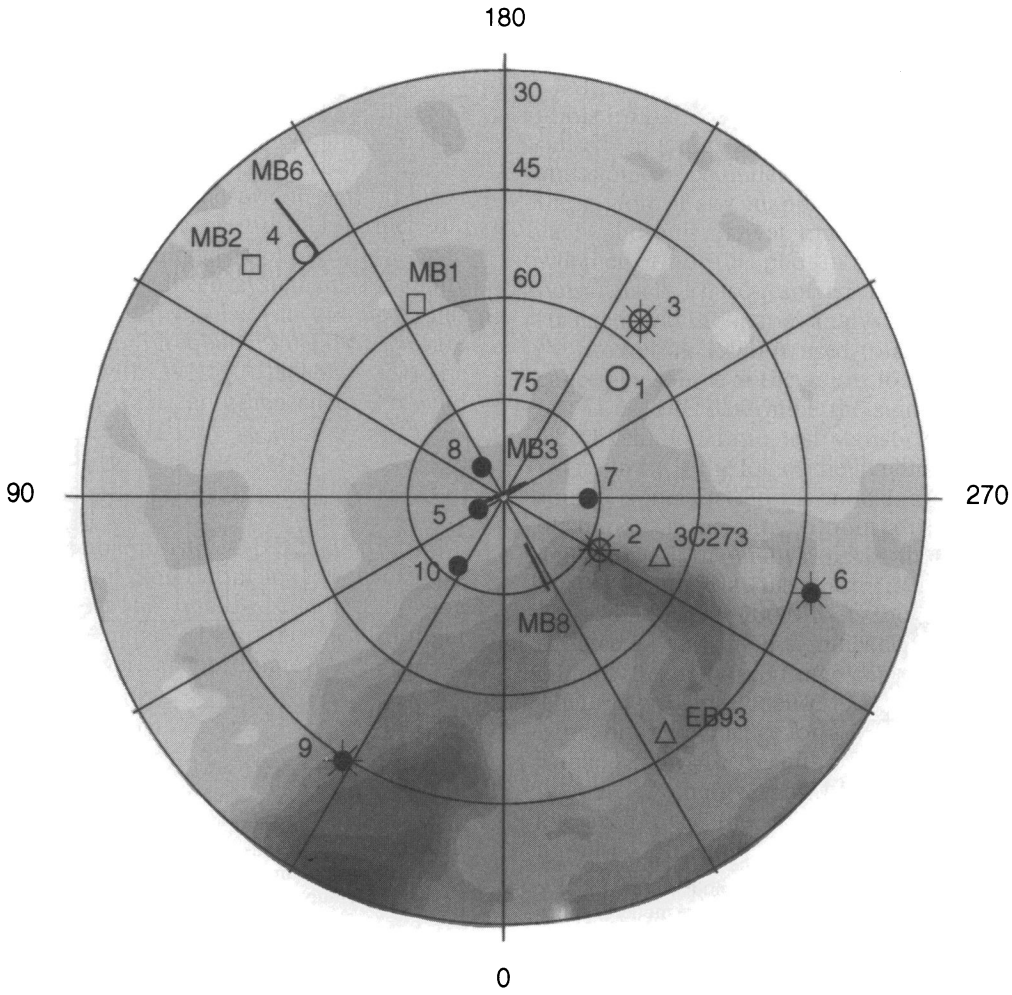

FIG. 4.—The region north of $b = 30°$, in Galactic coordinates, showing fields searched for diffuse coronal emission. *Open circles*: HUT large (19″ × 197″) aperture; *filled circles*: HUT small (10″ × 56″) aperture; *squares*: pointed targets of MB90, labeled with "MB" and the target number; *solid lines*: scanned targets of MB90; *triangles*: 3C 273 (Davidsen 1993) and EB93 (Edelstein & Bowyer 1993), two lines of sight discussed in the text. HUT targets showing O VI emission are marked with asterisks. Overplotted in grayscale is the *M*-band (490–1190 eV) X-ray intensity map of McCammon et al. (1983). The emission feature in the lower part of the figure is Radio Loop I.

may be more representative of the general halo. We will focus on this observation in our further analysis.

3. DISCUSSION

We begin this section with a brief survey of published observations of emission and absorption by hot gas in the halo. We consider the effects on the observed emission of gas and dust along the line of sight, then use these observations, together with our measured O VI flux, to constrain the properties of the O VI–emitting gas. Finally, we compare these results with the turbulent mixing layer models of Slavin, Shull, & Begelman (1993) and the Galactic fountain models of Benjamin & Shapiro (1996).

Martin & Bowyer (1990, hereafter MB90) detected diffuse C IV $\lambda\lambda$1548, 1551 and O III] $\lambda\lambda$1661, 1666 emission along a number of lines of sight through the Galactic halo (Fig. 4). The mean intensity of their C IV line is 6.4×10^{-8} ergs cm^{-2} s^{-1} sr^{-1}, well below our upper limits. Dixon et al. (1993) used HUT spectra from the Astro-1 mission to set limits on the O VI emission along six lines of sight. Their most sensitive observations yield a 2 σ upper limit of I(O VI) $\lesssim 1.1 \times 10^{-6}$ ergs cm^{-2} s^{-1} sr^{-1}. Edelstein & Bowyer (1993) observed the 7°.5 × 0°.1 field marked "EB93" in Figure 4, a line of sight that passes through a region of enhanced soft X-ray emission. They set a 90% confidence upper limit on the flux of the O VI λ1032 feature of 1.8×10^{-7} ergs cm^{-2} s^{-1} sr^{-1}. The upper limit for the total O VI flux is 1.5 times larger, or 2.7×10^{-7} ergs cm^{-2} s^{-1} sr^{-1}. Our O VI detection is greater than this limit, but lies along a different line of sight.

Shelton & Cox (1994) have reanalyzed the O VI absorption-line data of Jenkins (1978). Assuming a scale height of 3 kpc, they estimate the O VI column density perpendicular to the disk to be N(O VI) = 1.5×10^{14} cm^{-2}. Hurwitz et al. (1995) detect O VI absorption along the line of sight toward NGC 346 No. 1, a star in the Small Magellanic Cloud that does not appear on our map. They find N(O VI) $\leq 2 \times 10^{14}$ cm^{-2}. From a HUT spectrum of the quasar 3C 273 obtained on Astro-1, Davidsen (1993) sets a lower limit on the O VI column density of 3×10^{14} cm^{-2}. In Figure 4, we see that this line of sight also lies near Radio Loop I.

To what extent might halo emission in the O VI and C IV lines be attenuated by gas and dust along the line of sight? If the halo gas has a column density N(O VI) = 2×10^{14} cm^{-2} and a Doppler parameter $b = 20$ km s^{-1}, then its optical depth at line center (1032 Å) is $\tau_0 = 2$, making self-attenuation of the O VI emission a possibility. Resonance-

line absorption leads to scattering, however, and a gas of mixed absorbers and emitters is as likely to scatter photons into as out of the line of sight. Thus, we do not expect significant absorption of either O VI or C IV flux by the hot, collisionally excited gas.

A second effect may also be at work, however; photoionization of gas along the line of sight could produce a population of C^{+3} ions sufficient to attenuate the C IV flux, though substantial O^{+5} is not expected (Benjamin & Shapiro 1996). MB90 model a layer of absorbing material separate from and below the emitting region. They set an upper limit of 30% on the fraction of incident C IV radiation that could be removed from our line of sight by such a layer, an effect smaller than the uncertainty in our O VI fluxes (Table 2). As we are interested primarily in the relative O VI and C IV intensities, we will ignore resonance scattering in our analysis.

Scattering by dust is wavelength dependent. Because the UV extinction curve rises rapidly toward shorter wavelengths, observed O VI fluxes may be reduced relative to C IV along the same line of sight. We test the importance of this effect by considering the most heavily reddened line of sight in our survey, that toward NGC 4038, which has $E(B-V) = 0.013$ (Burstein & Heiles 1984). Using a Cardelli, Clayton, & Mathis (1989) extinction curve and assuming $R_V = 3.1$, we find that the reduction in the O VI flux, *relative to* C IV, is less than 10%, smaller than the uncertainties in our measured fluxes. We can thus safely ignore the effects of reddening in our analysis.

MB90 used their observed C IV intensities to estimate the electron density in the emitting gas. Shull & Slavin (1994) repeated this analysis using more recent atomic data and found that, for a homogeneous model with $4.7 \leq \log T \leq 5.3$, the data are consistent with $0.01 \leq n_e \leq 0.02$ cm^{-3} and $2200 \leq P/k \leq 3700$ cm^{-3} K. They derive an expression for the electron density in an O VI–emitting gas:

$$n_e = \frac{4\pi}{\langle \sigma v \rangle_e} \frac{I(\mathrm{O\ VI})}{N(\mathrm{O\ VI})} = (0.00799\ \mathrm{cm}^{-3}) \frac{I_{-7}(\mathrm{O\ VI})}{N_{14}(\mathrm{O\ VI})} \times \left[\frac{6}{\bar{\Omega}_{O6}(T)}\right] T_5^{1/2} \exp\left(\frac{1.392}{T_5}\right), \quad (1)$$

where $\langle \sigma v \rangle_e$ is the electron-impact excitation rate coefficient, I_{-7} the line intensity in units of 10^{-7} ergs cm^{-2} s^{-1} sr^{-1}, N_{14} the column density in units of 10^{14} cm^{-2}, and T_5 the gas temperature in 10^5 K. Expressions for $\langle \sigma v \rangle_e$ and $\bar{\Omega}_{O6}(T)$ (which equals 5.94 at $\log T = 5.5$) may be found in Shull & Slavin (1994). In Figure 5, we plot the electron density as a function of temperature for an O VI–emitting gas, assuming $N_{14}(\mathrm{O\ VI}) = 1.5$ (Shelton & Cox 1994) and $I_{-7} = 3.59$ (UGC 5675), and reproduce the results of Shull & Slavin for a C IV–emitting gas. Overplotted are lines of constant gas pressure, assuming $P/k = 1.92 n_e T$. We find that, for $5.3 \leq \log T \leq 5.8$, the data are consistent with $n_e \approx 0.06$ cm^{-3} and $22{,}000 \leq P/k \leq 67{,}000$ cm^{-3} K. The electron density derived for the O VI–emitting gas is nearly an order of magnitude greater than that derived for C IV. Raising $N_{14}(\mathrm{O\ VI})$ to 3.0 (Davidsen 1993) reduces n_e by a factor of 2, still several times the C IV value. This result argues against simple models that postulate a uniform gas at a single temperature.

Shull & Slavin (1994) present a model in which turbulent mixing layers and isobarically cooling supernova remnants provide significant amounts of halo gas at about $10^{5.3}$ K. Turbulent mixing layers have been investigated by Begelman & Fabian (1990) and Slavin et al. (1993). In Figure 6, we plot the line ratio $I(\mathrm{O\ VI})/I(\mathrm{C\ IV})$ predicted by Slavin et al. for values of $\bar{T}$, the temperature attained by the gas immediately after mixing, between $10^{5.0}$ and $10^{5.5}$ K, and v,

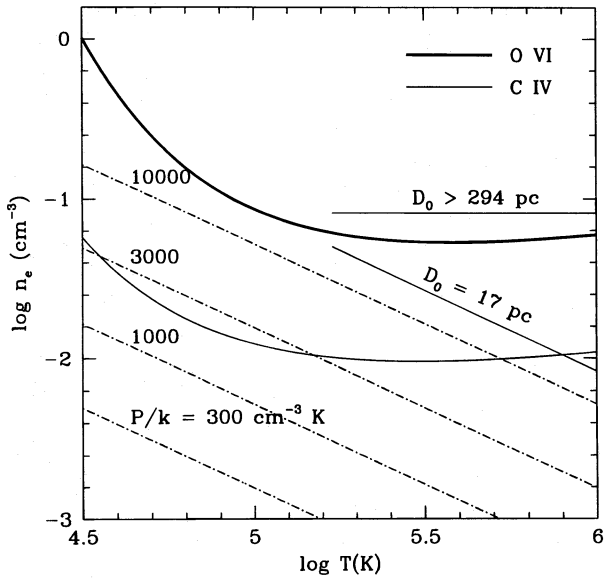

FIG. 5.—The electron density n_e as a function of temperature for an O VI emitting gas (*thick curve*), assuming $N_{14}(\mathrm{O\ VI}) = 1.5$ (Shelton & Cox 1994) and $I_{-7} = 3.59$ as found in the HUT spectrum of UGC 5675. We reproduce the results of Shull & Slavin (1994) for a C IV emitting gas (*thin curve*). Overplotted are lines of constant gas pressure ($P/k = 1.92\ n_e T$; *dot-dashed lines*). Also plotted are two lines connecting the electron densities predicted for log $T = 5.2$ and 6.0 gas in the largest ($D_0 > 294$ pc) and smallest ($D_0 = 17$ pc) clouds modeled by Benjamin & Shapiro (1996). The largest clouds are isochoric, so n_H is constant as they cool. Throughout this temperature regime, our derived n_e curve lies within the predicted limits.

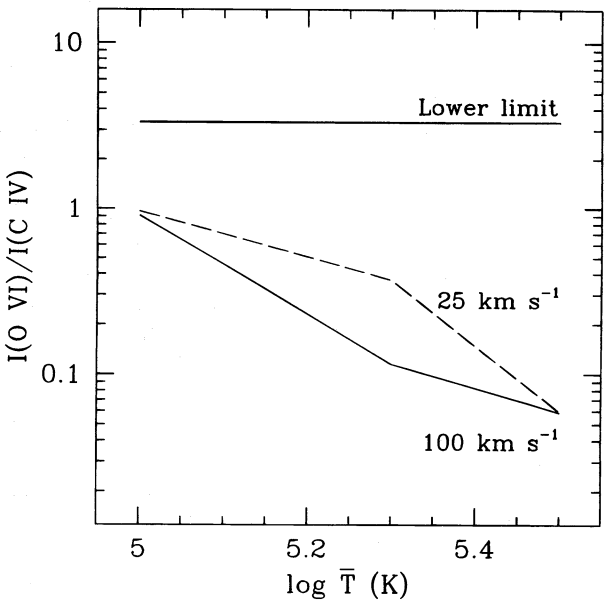

FIG. 6.—The $I(\mathrm{O\ VI})/I(\mathrm{C\ IV})$ ratio predicted by the Slavin et al. (1993) turbulent mixing layer models as a function of $\bar{T}$, the temperature of the gas immediately after mixing, and v, the velocity of the hot gas penetrating the mixing layer. Our lower limit on $I(\mathrm{O\ VI})/I(\mathrm{C\ IV})$ is significantly higher than predicted for all values of $\bar{T}$. Slavin et al. prefer a value of log $\bar{T} = 5.3$ for the Galactic halo. Turbulent mixing layers at this temperature can account for less than 10% of the O VI emission from the Galactic halo.

the velocity of the hot gas penetrating the mixing layer, of 25 and 100 km s^{-1}. The authors prefer a value of log $\bar{T}$ = 5.3; at this temperature, their models reproduce the I(C IV)/I(O III]) ratio observed by MB90. Using the O VI line flux and C IV upper limit determined from the HUT spectrum of UGC 5675, we find that I(O VI)/I(C IV) $\geq$ 3.36. This limit is significantly higher than the Slavin et al. predictions for all values of $\bar{T}$ and implies that turbulent mixing layers with log $\bar{T}$ = 5.3 contribute less than 10% of the O VI emission from the Galactic halo.

Shapiro & Benjamin (1991, 1993) and Benjamin & Shapiro (1993, 1996) model hot gas cooling radiatively from a temperature near 10^6 K in a one-dimensional, planar, steady state flow model of a Galactic fountain. Edgar & Chevalier (1986) found such simple models unable to reproduce simultaneously the C IV, Si IV, and N V column densities observed through the Galactic halo, but by including the effects of self-ionization (photoionization by radiation emitted by the flow itself), Benjamin & Shapiro are able to raise the predicted C IV and Si IV column densities to the observed values. Their models predict I(O VI)/I(C IV) $\approx$ 9–11, values consistent with our lower limit. After O VI and C IV, the strongest predicted lines in the HUT range (and well separated from Lyα) are C III λ977 and He II λ1640. Our upper limits to I(C III)/I(C IV) and I(He II)/I(C IV) (assuming the mean C IV intensity of MB90) lie well above the predicted ratios.

In the cooling-flow models of Benjamin & Shapiro (1996), hot gas cooling in the halo is expected to exhibit a range of temperatures, densities, and pressures. The cooling history of the gas is determined by the initial length scale of the cooling region, D_0. For large D_0, i.e., $D_0 > 294$ pc, the gas density is initially $n_{H,0} = 6.8 \times 10^{-2}$ cm^{-3} and remains constant during the evolution of the flow. For the smallest allowed scale, $D_0 = 17$ pc, the initial gas density is $n_{H,0} = 6.9 \times 10^{-3}$ cm^{-3}, and the gas cools at constant pressure until log $T \approx 5.2$. Assuming that $n_e = 1.2 n_H$, we display these predictions (somewhat crudely) as straight lines in Figure 5. At log T = 5.5, the peak of the O VI emissivity curve (Landini & Monsignori Fossi 1990), our derived n_e curve lies within the predicted limits.

How do we explain the discrepancy between the O VI and C IV electron densities? According to Benjamin & Shapiro (1996), C^{+3} ions are present in two phases of the cooling gas, each of which contributes differently to the observed absorption and emission line strengths. The emission comes predominantly from hot, collisionally ionized gas cooling from $T = 10^{5.5}$ to $10^{4.5}$ K, while the absorption occurs both in this gas and in photoionized gas at about 10^4 K. This cooler material raises the observed C IV column density without contributing to the net C IV flux, skewing estimates of n_e. Because O^{+5} ions arise primarily through collisional ionization rather than photoionization, the O VI emission provides an unambiguous probe of conditions in the hot gas. Observations of I(O VI) and N(O VI) along the same lines of sight will be required to test fully theories of the cooling processes in the Galactic halo.

4. CONCLUSIONS

We have searched spectra obtained along 10 lines of sight at high Galactic latitude with the Hopkins Ultraviolet Telescope for far-UV emission from coronal gas. Of four spectra obtained through a 19″ × 197″ aperture, two show O VI $\lambda\lambda$1032, 1038 emission at a significance of 4 σ. Two of six spectra taken through a 10″ × 56″ aperture show O VI emission, though at only 2 σ significance. The detection of O VI emission suggests the presence in the Galactic halo of gas cooling from a high temperature (log $T \gtrsim 5.5$), whether via mixing layers or a self-photoionizing fountain. None of the spectra exhibit significant emission from C IV $\lambda\lambda$1548, 1551, though our upper limits lie well above previous detections (MB90). Three of the four lines of sight along which O VI is detected lie on or near Radio Loop I. We have used the O VI flux and C IV limit from the fourth to set a limit on I(O VI)/I(C IV). The result is consistent with the predictions of the Galactic fountain models of Benjamin & Shapiro (1996), but not with the turbulent mixing layer models of Slavin et al. (1993) for 5.0 $\leq$ log $\bar{T} \leq$ 5.5. Combining our measured O VI intensity with estimates of N(O VI) through the halo, we calculate n_e and P/k as a function of temperature; our results are higher than those based on C IV measurements, but consistent with self-photoionizing models of the cooling gas. Observations of both species along the same lines of sight will be required to constrain more tightly the dynamic and cooling histories of the coronal gas in the Galactic halo.

We thank R. Benjamin for helpful discussions and R. Benjamin and P. Shapiro for providing results prior to publication. This research has made use of the NASA/IPAC Extragalactic Database (NED), which is operated by the Jet Propulsion Laboratory, Caltech, under contract with the National Aeronautics and Space Administration, the NASA ADS Abstract Service, and the Catalogue Service of the CDS, Strasbourg, France. We wish to acknowledge the efforts of our colleagues on the HUT team as well as the many NASA personnel who helped make the Astro-2 mission successful. The Hopkins Ultraviolet Telescope Project is supported by NASA contract NAS 5-27000 to the Johns Hopkins University.

REFERENCES

Avni, Y. 1976, ApJ, 210, 642
Begelman, M. C., & Fabian, A. C. 1990, MNRAS, 244, 26P
Benjamin, R. A., & Shapiro, P. R. 1993, in UV and X-Ray Spectroscopy of Astrophysical and Laboratory Plasmas, ed. E. H. Silver & S. M. Kahn (Cambridge: Cambridge Univ. Press), 280
———. 1996, ApJS, submitted
Blair, W. P., Long, K. S., Vancura, O., & Holberg, J. B. 1991, ApJ, 374, 202
Bregman, J. N. 1980, ApJ, 236, 577
Burstein, D., & Heiles, C. 1984, ApJS, 54, 33
Cardelli, J. A., Clayton, G. C., & Mathis, J. S. 1989, ApJ, 345, 245
Davidsen, A. F. 1993, Science, 259, 327
Davidsen, A. F., et al. 1992, ApJ, 392, 264
Dixon, W. V., Davidsen, A. F., Bowers, C. W., Kriss, G. A. Kruk, J. W., & Ferguson, H. C. 1993, in AIP Conf. Proc. 278, Back to the Galaxy, ed. S. S. Holt & F. Verter (New York: AIP), 528
Edelstein, J., & Bowyer, S. 1993, Adv. Space Res., 13(12), 307
Edgar, R. J., & Chevalier, R. A. 1986, ApJ, 310, L27
Feldman, P. D. 1995, private communication
Feldman, P. D., et al. 1992, Geophys. Res. Lett., 19, 453
Green, D. A. 1991, PASP, 103, 209
Hartigan, P., Raymond, J., & Hartmann, L. 1987, ApJ, 316, 323
Heiles, C., Chu, Y.-H., Reynolds, R. J., Yegingil, I., & Troland, T. H. 1980, ApJ, 242, 533
Hurwitz, M., Bowyer, S., Kudritzki, R.-P., & Lennon, D. J. 1995, ApJ, 450, 149
Iwan, D. 1980, ApJ, 239, 316
Jenkins, E. B. 1978, ApJ, 219, 845
Kriss, G. A. 1994, in ASP Conf. Ser. 61, Astronomical Data Analysis Software and Systems III, ed. D. R. Crabtree, R. J. Hanisch, & J. Barnes (San Francisco: ASP), 437
Kruk, J. W., Durrance, S. T., Kriss, G. A., Davidsen, A. F., Blair, W. P., Espey, B. R., & Finley, D. 1995, ApJ, 454, L1

Landini, M., & Monsignori Fossi, B. C. 1990, A&AS, 82, 229
Lauberts, A., & Valentijn, E. A. 1989, The Surface Photometry Catalogue of the ESO-Uppsala Galaxies (Munich: ESO)
Martin, C., & Bowyers, S. 1990, ApJ, 350, 242 (MB90)
McCammon, D., Burrows, D. N., Sanders, W. T., & Kraushaar, W. L. 1983, ApJ, 269, 107
McKee, C. F. 1993, in AIP Conf. Proc. 278, Back to the Galaxy, ed. S. S. Holt & F. Verter (New York: AIP), 499
Norman, C., & Ikeuchi, S. 1989, ApJ, 345, 372
Savage, B. D., Lu, L., Weymann, R. J., Morris, S. L., & Gilliland, R. L. 1993, ApJ, 404, 124
Sembach, K., & Savage, B. D. 1992, ApJS, 83, 147
Shapiro, P. R., & Benjamin, R. A. 1991, PASP, 103, 923
———. 1993, in Star Formation, Galaxies, and the Interstellar Medium, ed. J. Franco, F. Ferrini, & G. Tenorio-Tagle (Cambridge: Cambridge Univ. Press), 275
Shapiro, P. R., & Field, G. B. 1976, ApJ, 205, 762
Shelton, R. L., & Cox, D. P. 1994, ApJ, 434, 599
Shull, J. M., & Slavin, J. D. 1994, ApJ, 427, 784
Slavin, J. D., Shull, J. M., & Begelman, M. C. 1993, ApJ, 407, 83
Spitzer, L. 1956, ApJ, 124, 20
Voit, G. M., Donahue, M., & Slavin, J. D. 1994, ApJS, 95, 87